Physica B 449 (2014) 138–143

Contents lists available at ScienceDirect

Physica B

journal homepage: www.elsevier.com/locate/physb

Structural and large magnetocaloric properties of $La_{0.67-x}Y_xBa_{0.23}Ca_{0.1}MnO_3$ perovskites ($0 \leq x \leq 0.15$)

Mounira Abassi [a,*], N. Dhahri [a], J. Dhahri [a], E.K. HLIL [b]

[a] Laboratoire de la Matière Condensée et des Nanosciences, Département de Physique, Faculté des Sciences de Monastir 5019, Tunisie
[b] Institut Néel, CNRS et Université Joseph Fourier, BP 166, F-38042 Grenoble cedex 9, France

ARTICLE INFO

Article history:
Received 8 April 2014
Accepted 5 May 2014
Available online 17 May 2014

Keywords:
Perovskite oxides
Yttrium doping
Curie temperature
Magnetic entropy change

ABSTRACT

$La_{0.67}Ba_{0.23}Ca_{0.1}MnO_3$ doped with different amounts of yttrium (Y) result in the series $La_{0.67-x}Y_xBa_{0.23}Ca_{0.1}MnO_3$ (LYBCMO) (x=0.00, 0.05, 0.10 and 0.15) which was synthesized by conventional solid state ceramics route. All samples show a rhombohedral structure (space group $R\overline{3}c$) at room temperature. A transition from a paramagnetic to a ferromagnetic phase is observed at Curie temperature, T_C. It has been found that the substitution of Y on the La site causes a reduction in T_C. Analyses of crystallographic data suggested a strong correlation between structural properties and magnetism. As an example, a relationship between the distortion of MnO_6 octahedron and the reduction in Curie temperature. The magnetic entropy change ($-\Delta S_m$) was estimated from isothermal magnetization curves. It decreases from 4.91 J/kg K at 350 k (x=0.00) to 4.14 J/kg K at 289 K (x=0.15) with the increase of Y content under $\mu_0H=5$ T. The relative cooling power (RCP) is found to be 365 J/kg for $La_{0.67}Ba_{0.23}Ca_{0.1}MnO_3$ and 288 J/kg for $La_{0.52}Y_{0.15}Ba_{0.23}Ca_{0.1}MnO_3$ in the magnetic field change of 5 T. From these results, $La_{0.67-x}Y_xBa_{0.23}Ca_{0.1}MnO_3$ materials are strongly suggested for use as active refrigerants in magnetic refrigeration technology at near room temperature.

1. Introduction

Mixed valence manganites with perovskite structure have been studied for more than 50 years due to the interesting interplay between electronic and magnetic features. While pure $LaMnO_3$ is an antiferromagnetic insulator, the doping on the La-site gives rise to a mixed valence of $Mn^{3+}(t_{2g}^3e_g^1)$ and $Mn^{4+}(t_{2g}^3)$ out of which the e_g electrons can be delocalized. This is due to their strong hybridization with oxygen 2p states. Therefore they can mediate the ferromagnetic interaction between localized t_{2g} spins. The effective interaction between the antiferromagnetic super exchange coupling and ferromagnetic double exchange gives rise to various magnetic structures [1,2]. The simultaneous magnetic transition and discontinuous volume variation at Curie temperature (T_C) can strongly influence the magnetic entropy change [3,4]. They are found to be comparable with the changes observed in other solid magnetic refrigerants [5,6]. The magnetocaloric effect (MCE) describing the reduction in the magnetic part of the total entropy upon adiabatic magnetization is an intrinsic property of all magnetic materials. The MCE is used in magnetic refrigeration technology because of the strong demand for materials with giant MCE for use as magnetic refrigerants. The possibility of using magnetic refrigeration in both near room temperature and cryogenic temperature regime has led to much research in the field of MCE [7,8]. For a long time, pure Gadolinium (Gd) has been considered as the most prominent magnetic refrigerant for use in room temperature magnetic refrigerators because of its large magnetic entropy change around 294 K for $\mu_0H=5$ T [9]. However, the high price of Gd (~4000 $/kg) deprives us from using it in actual application. Therefore, the search for a new, cheaper working substance with large MCE becomes a main research topic in this field. At present, these are some possible candidates: $Gd_5(Si_{1-x}Ge_x)_4$ [10], $MnFeP_{1-x}As_x$ [11], $MnAs_{1-x}Sb_x$ [12] and $Mn_{1-x}Fe_xAs$ [13]. Hence, manganites are interesting for application as potential candidates in magnetic refrigeration [14,15]. The advantages of manganites are their high chemical stability, low eddy current heating, high resistivity, low cost, and tunable T_C. Therefore, a refrigeration unit composed of several manganites with different T_C can be spanned over a wide range of temperature (namely, 240–340 K). Generally, in manganites, the large magnetic entropy change could be attributed to the variation of the double exchange interaction between Mn^{3+} and Mn^{4+} ions and the strong spin lattice coupling [16].

In the present study, we investigate the structure, magnetic and magnetocaloric effect related to the effects of Y doping in $La_{0.67-x}Y_xBa_{0.23}Ca_{0.1}MnO_3$, which can be a suitable candidate as a

---

* Corresponding author.
E-mail address: mouniraabassi90@yahoo.com (M. Abassi).

http://dx.doi.org/10.1016/j.physb.2014.05.006

working substance in magnetic refrigeration at near room temperature.

2. Experimental details

A series of $La_{0.67-x}Y_xBa_{0.23}Ca_{0.1}MnO_3$ ($0 \le x \le 0.15$) polycrystalline samples has been prepared using the standard solid-state reaction method in air. Stoichiometric quantities of high-purity oxides–carbonates La_2O_3, Y_2O_3, $BaCO_3$, $CaCO_3$ and MnO_2 were thoroughly mixed and ground. Then they were heated at 1273 K for 24 h with intermediate grinding, they reacted at 1423 K for 24 h. Subsequently, they were pressed into pellets. A final sintering was carried out at 1673 K for 48 h. The structure was characterized, at room temperature, by X-ray powder diffractometer with Co $K\alpha$ radiations ($\lambda = 1.789$ Å). The analysis phase was carried out using FULLPROF program based on the Rietveld method [17]. Data for the Rietveld refinement were collected in the 2θ range 10–100° with a step size of 0.02° and a counting time of 18 s per step.

Scanning electron microscope (SEM) was used to determine the grain size and the morphology of the samples. The magnetization measurements versus temperature and versus field were carried out using a BS2 magnetometer developed in Louis Neel Laboratory of Grenoble.

3. Results and discussion

3.1. Scanning electron microscopy SEM

From the analysis of SEM images, the average grain size for all the samples was found to be between 293 and 105 nm for $x=0.00$ and $x=0.15$, respectively. Thus observing a good intergranular connection (inset Fig. 1b, for $x=0.10$). In fact, we can also calculate the average grain size (T_G) from the XRD peaks using the Scherrer formula

$$T_G = \frac{0.9\lambda}{\beta \cos \theta} \tag{1}$$

where λ is the X-ray wavelength employed, θ is the diffraction angle for the most intense peak (104), and β is defined as $\beta^2 = \beta_m^2 - \beta_s^2$. Here β_m is the experimental full width at half maximum (FWHM) and β_s is the FWHM of a standard silicon sample [18]. The as obtained (T_G) are estimated to vary from 98 to 35 nm for $x=0.00$ and $x=0.15$, respectively. These values are significantly smaller than the ones determined by SEM. This is because observations by imaging techniques such as SEM often give the size of the secondary particles and the X-ray line broadening analysis discloses the size of primary particles.

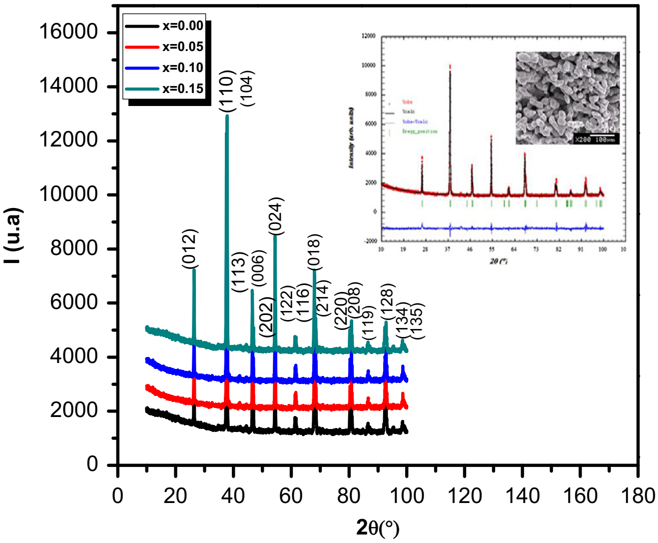

Fig. 1. Room temperature powder XRD patterns for $La_{0.67-x}Y_xBa_{0.23}Ca_{0.1}MnO_3$ ($0 \le x \le 0.15$) compounds with indexing in the rhombohedral $R\overline{3}c$ space group. The inset-a shows the Ritveld plots of XRD data for LYBCMO ($x=0.10$) compound and the inset-b represents the SEM micrographs for LYBCMO.

3.2. Structural properties

Phase identification and structural analysis were carried out by X-ray diffraction (XRD). The refinement of the XRD patterns of $La_{0.67-x}Y_xBa_{0.23}Ca_{0.1}MnO_3$ ($x=0.00$, 0.05, 0.10 and 0.15) compounds has revealed that all samples are single phase with no detectable secondary phase within the XRD limits (Fig. 1). These compounds were found to crystallize in the rhombohedral structure with $R\overline{3}c$ space group. The inset of Fig. 1a examplifies the Rietveld refinement XRD profile for LYBCMO sample ($x=0.10$). Refined cell parameters and cell volume are given in Table 1. In this table the structure factor R_F and the goodness of fit χ^2 are also reported. The structure parameter values determined for LYBCMO compound are in good agreement with those reported in the literature [19]. With increasing yettruim concentration, the lattice parameters change in a continuous manner indicating perfect solid solubility of Y at La site. The unit-cell volume decreases with increasing Y substitution. A decrease in the rhombohedra lattice volume with an increase in yttrium content from $x=0.00$ to $x=0.15$ is explained by the replacement of La^{3+}ions ($r=1.216$ Å) by smallerY^{3+} ions ($r=1.06$ Å) [20]. This is confirmed by the Rietveld refinement of the Mn–O bond length and the Mn–O–Mn bond angles calculated from the structural parameters (Table 1). From the results of the average distances Mn–O and the average angles Mn–O–Mn, it is considered that each MnO_6 octahedron has a small distortion. Accordingly, the lattice distortion is caused by the partial replacement of La by Y which is governed by the tolerance factor ($t = r_{La,Y,Ba,Ca} + r_O/\sqrt{2}(r_{Mn} + r_O)$); geometric measure of size mismatch of the perovskites [21]. Oxide based manganite compounds have a perovskite structure if their tolerance factor lies in the limits of $0.75 < t < 1$. In an ideal case the value must be equal to unity. As the calculated values of (t) of all the samples of the present investigation are within range (Table 1), one may conclude that they might have a stable perovskite structure. What is interesting to note from Table 1 is that (t) values increase continuously with the increase of the ionic radius of A-site.

Table 1
Refined structural parameters for $La_{0.67-x}Y_xBa_{0.23}Ca_{0.1}MnO_3$ ($0 \le x \le 0.15$) at room temperature.

	x			
	0.00	0.05	0.10	0.15
$R\overline{3}c$ **phase**				
a (Å)	5.5740(1)	5.5450 (2)	5.5430(1)	5.5400(3)
c (Å)	13.4800(1)	13.4779(2)	13.4750(2)	13.4693(3)
V (Å^3)	359.25(3)	358.88(1)	358.54	358.10(4)
(La/Y)B_{iso} (Å^2)	0.268(4)	0.133(6)	0.114(3)	0.448(2)
(Mn)B_{iso} (Å^2)	0.380(5)	0.7521(7)	0.6251(1)	0.5446(2)
(O)B_{iso} (Å^2)	1.756(7)	1.3391(6)	1.5428(6)	1.5722(3)
X(O)	0.453(7)	0.4470(6)	0.5428(2)	0.5722 (1)
d_{Mn-O} (Å)	1.9746(2)	1.9766(4)	1.9800(1)	1.9849(7)
$\theta_{Mn-O-Mn}$ (°)	163.76(6)	162.81(4)	161.93(8)	159.96(2)
t	0.9377	0.9347	0.9315	0.9278
σ^2 ($\times 10^{-3}$ Å^2)	0.0084	0.0073	0.0063	0.0054
Discrepancy factors				
R_{wp} (%)	3.17	3.02	3.35	3.65
R_p (%)	2.4	2.31	2.46	2.71
R_F (%)	6.09	8.27	6.31	8.40
χ^2 (%)	1.50	1.22	1.5	1.98